Cell

RNF168 Binds and Amplifies Ubiquitin Conjugates on Damaged Chromosomes to Allow Accumulation of Repair Proteins

Carsten Doil,[1] Niels Mailand,[1] Simon Bekker-Jensen,[1] Patrice Menard,[1] Dorthe Helena Larsen,[1] Rainer Pepperkok,[2] Jan Ellenberg,[3] Stephanie Panier,[4] Daniel Durocher,[4] Jiri Bartek,[1] Jiri Lukas,[1,*] and Claudia Lukas[1]

[1]Institute of Cancer Biology and Centre for Genotoxic Stress Research, Danish Cancer Society, Strandboulevarden 49, DK-2100 Copenhagen, Denmark

[2]Cell Biology/Biophysics Units

[3]Gene Expression Unit

European Molecular Biology Laboratory (EMBL), Meyerhofstrasse 1, D-69117 Heidelberg, Germany

[4]Samuel Lunenfeld Research Institute, Mount Sinai Hospital, 600 University Avenue, Toronto, Ontario M5G 1X5, Canada

*Correspondence: jil@cancer.dk

DOI 10.1016/j.cell.2008.12.041

SUMMARY

DNA double-strand breaks (DSBs) not only interrupt the genetic information, but also disrupt the chromatin structure, and both impairments require repair mechanisms to ensure genome integrity. We showed previously that RNF8-mediated chromatin ubiquitylation protects genome integrity by promoting the accumulation of repair factors at DSBs. Here, we provide evidence that, while RNF8 is necessary to trigger the DSB-associated ubiquitylations, it is not sufficient to sustain conjugated ubiquitin in this compartment. We identified RNF168 as a novel chromatin-associated ubiquitin ligase with an ability to bind ubiquitin. We show that RNF168 interacts with ubiquitylated H2A, assembles at DSBs in an RNF8-dependent manner, and, by targeting H2A and H2AX, amplifies local concentration of lysine 63-linked ubiquitin conjugates to the threshold required for retention of 53BP1 and BRCA1. Thus, RNF168 defines a new pathway involving sequential ubiquitylations on damaged chromosomes and uncovers a functional cooperation between E3 ligases in genome maintenance.

INTRODUCTION

Following the generation of DNA double-strand breaks (DSBs), the neighboring chromatin undergoes extensive modifications initiated by ATM-dependent phosphorylation of histone H2AX (γ-H2AX) and culminating at the generation of a distinct compartment capable of retaining various genome caretakers (Fernandez-Capetillo et al., 2004; Lukas et al., 2004b). Several lines of evidence suggest that the main function of the DSB-induced chromatin modifications (and the resulting concentration of proteins in this compartment) is to enhance the efficiency of repair and signaling reactions, especially under conditions that pose increased demand on genome surveillance (Celeste et al., 2003). This concept has gained significant support from studies showing that a forced tethering of DSB regulators to chromatin was sufficient to induce checkpoint signaling and delay cell-cycle progression even without the concomitant DNA damage (Bonilla et al., 2008; Soutoglou and Misteli, 2008).

Recent work provided important mechanistic insights into the role of posttranslational modifications in the hierarchical protein assembly on damaged chromatin. The central coordinating factor appears to be MDC1, a large adaptor protein, which through its BRCT domains directly binds phosphorylated S139 of γ-H2AX (Stucki et al., 2005) and is among the first proteins to arrive at the DSB sites (Lukas et al., 2004a). Importantly, MDC1 not only senses the most proximal DSB-associated phosphorylation events (γ-H2AX), but it also integrates distinct types of constitutive, as well as DNA damage-induced, signaling and thereby orchestrates the ensuing protein assemblies at the DSB sites. Thus, constitutive phosphorylation of the S-D-T clusters by Casein kinase 2 generates binding sites for the FHA and BRCT domains of NBS1, a core component of the MRE11-NBS1-RAD50 nuclease complex (Melander et al., 2008; Spycher et al., 2008). At the same time, MDC1 integrates also the bona fide DNA damage signaling through the ATM-dependent phosphorylation of a cluster of S/T-Q residues, which generate a landing platform for RNF8, an FHA-containing ubiquitin ligase. RNF8 catalyzes local histone ubiquitylation and thereby renders the DSB-flanking chromatin permissive to assemble additional DSB regulators such as 53BP1 and BRCA1 (Huen et al., 2007; Kolas et al., 2007; Mailand et al., 2007; Sobhian et al., 2007; Wang et al., 2007; Wang and Elledge, 2007; Yan et al., 2007). Finally, in addition to phosphorylations and ubiquitylations, other posttranslational modifications contribute to the full-scale development of this compartment. It has been shown that the TRRAP/TIP60 histone acetyltransferase facilitates 53BP1 and BRCA1 retention at the DSB sites (Murr et al., 2006), and one report suggested that TIP60 is functionally linked with histone ubiquitylations (Ikura et al., 2007). How all of these

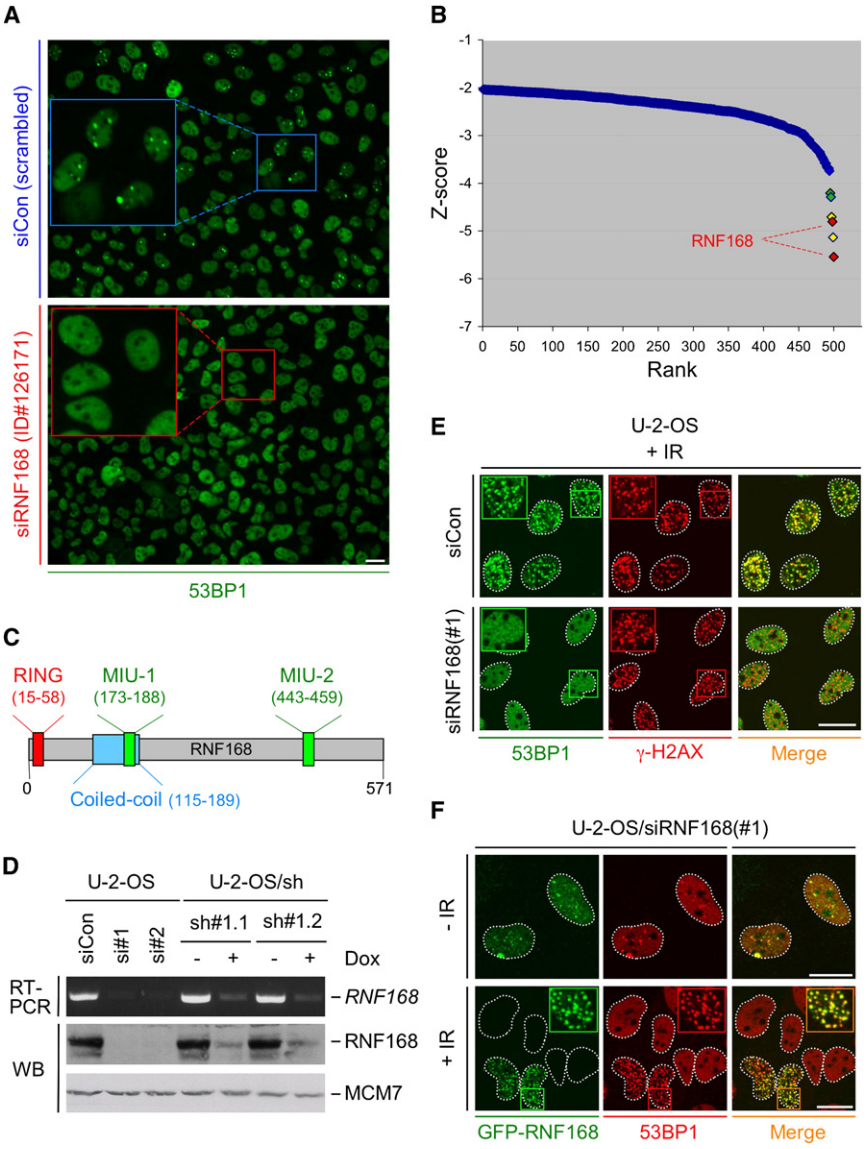

Figure 1. RNF168 Regulates Retention of 53BP1 at the DNA Damage-Modified Chromatin

(A) Representative fields from the siRNA arrays showing cell populations cultured for 3 days on spots containing control (siCon) or RNF168-targeting siRNAs and immunostained with an antibody to 53BP1. The siRNA ID number specifies the oligonucleotide in the Ambion siRNA database (http://www4.appliedbiosystems.com/tools/workflow/workflow.php).

(B) A scatter plot of Z scores derived from the RNAi screen for regulators of 53BP1 retention at spontaneous nuclear foci. The plotted values show the area of the least incidence of 53BP1 foci. The positions of RNF168 as the two high-scoring hits are indicated (red). MDC1 (yellow) and RNF8 (green) are indicated as positive controls.

(C) A schematic structure of RNF168 (Ensembl gene ID: ENSG00000163961).

(D) U-2-OS cells were treated with a control siRNA (siCon) or two siRNAs (si#1 or si#2) targeting distinct regions of RNF168 mRNA (left). Alternatively, two U-2-OS cell lines (sh#1.1, sh#1.2) conditionally expressing an RNF168-targeting shRNA were induced or not with Doxycycline (Dox) and incubated for 2 days (right). RNA and proteins were extracted and subjected to RT-PCR (top) and western blot (WB) analysis (bottom). MCM7 immunoblot is a loading control.

(E) U-2-OS cells were treated with the indicated siRNAs, incubated for 2 days, subjected to IR (3 Gy), and 1 hr later immunostained with the indicated antibodies.

(F) U-2-OS cells were treated with the RNF168-targeting siRNA (si#1) for 24 hr, transfected with the expression plasmid for RNAi-resistant GFP-RNF168, incubated for 24 hr, irradiated as in (E), and immunostained with an antibody to 53BP1. Scale bars, 10 μm.

processes are coordinated in space and time is a major challenge for future research.

To gain new insights into these issues, we performed a high-content microscopy screen for genes whose downregulation by RNA interference (RNAi) prevents accumulation of 53BP1 at the sites of DSBs. Retention of 53BP1 on chromatin requires all major chromatin modifications (H2AX phosphorylation, RNF8-mediated ubiquitylation, and TRRAP/TIP60-dependent acetylation) induced by DNA damage. Furthermore, accumulation of 53BP1 at DSBs requires also constitutive epigenetic marks (such as dimethylated K79 of histone H3 and/or dimethylated K20 of histone H4), which are recognized by the Tudor domain of 53BP1 (Botuyan et al., 2006; Huyen et al., 2004). Thus, 53BP1 integrates a multitude of upstream events, which makes it particularly suitable to screen for hitherto unknown factors involved in genome surveillance. Here, we mine this screen and identify RNF168, a protein that combines E3 ubiquitin ligase activity with an ability to bind conjugated ubiquitin on damaged chromosomes and mechanistically defines a molecular pathway involved in the DNA damage-induced chromatin response.

RESULTS

Identification of RNF168 as a Novel Factor Required for 53BP1 Accumulation on Damaged Chromosomes

Using previously developed methods for microscopy-based high-throughput RNAi screening (Erfle et al., 2007) combined with a custom-designed readout for 53BP1 focus formation (see Supplemental Experimental Procedures and Figures S1A–S1G available online), we identified RNF168 as one of the strongest hits that inhibited focal accumulation of 53BP1 on chromatin (Figure 1A). This inhibition was achieved by independent siRNA oligonucleotides and was as robust as the effect of MDC1 or RNF8, two known regulators of 53BP1 retention at

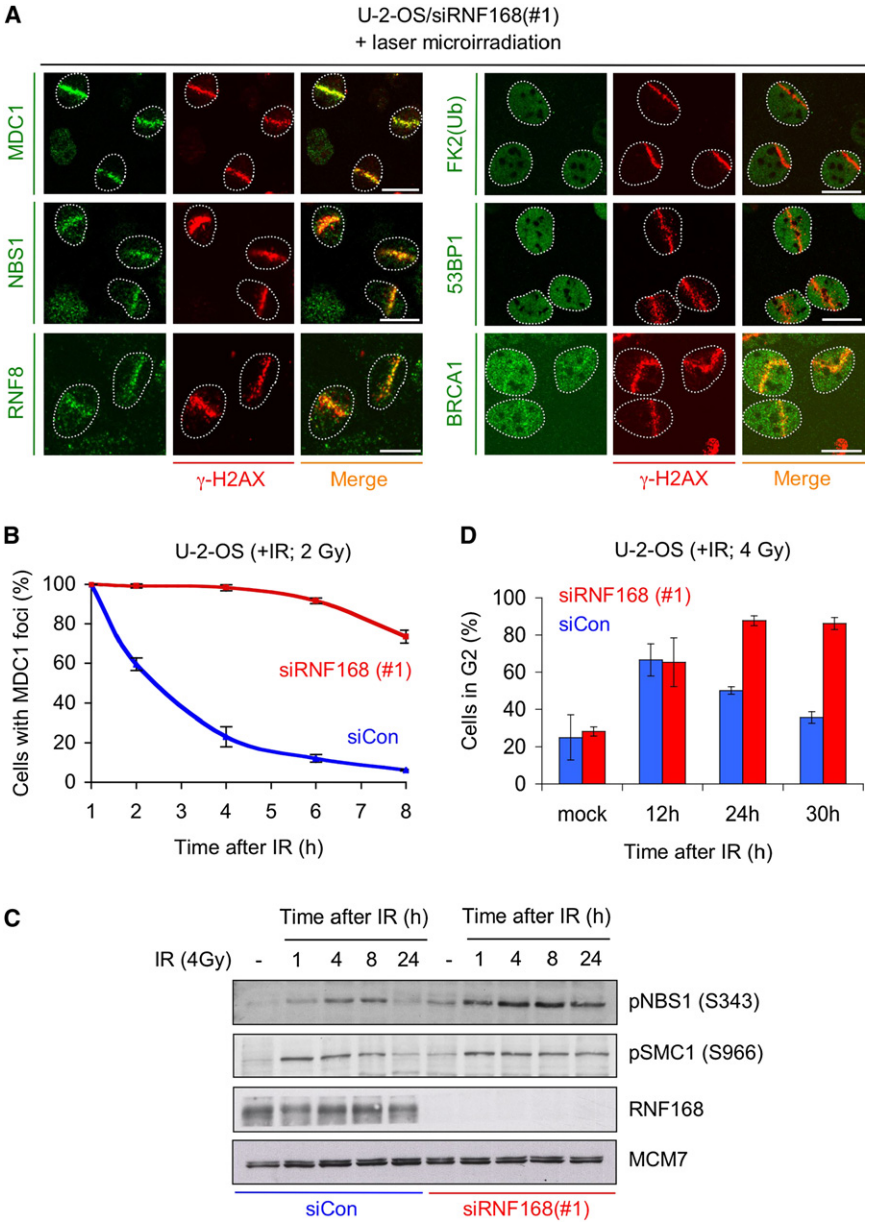

Figure 2. Knockdown of RNF168 Impairs Cellular Responses to DSBs

(A) U-2-OS cells were treated with the RNF168-targeting siRNA for 2 days, microirradiated by the laser, and 1 hr later immunostained with the indicated antibodies. At least 100 cells were microirradiated for each condition and yielded consistent results. Scale bars, 10 μm.

(B) U-2-OS cells were treated with the RNF168-targeting (#1) or control (siCon) siRNAs for 2 days, exposed to IR (2 Gy), and at the indicated time points immunostained with an antibody to MDC1. The nuclei where the number of MDC1 foci exceeded the background level (10 foci per nucleus) were counted. The graph is a summary from two experiments and shows the percentage of cells with IR-induced MDC1 foci relative to the starting point (1 hr after IR); 400 cells were scored for each time point. Error bars, SE.

(C) U-2-OS cells were treated as in (B), exposed to IR (4 Gy), and at the selected time points analyzed by immunoblotting with the indicated phospho-specific antibodies. The immunoblots for total RNF168 and MCM7 are controls for RNAi efficiency and equal loading, respectively.

(D) U-2-OS cells were treated and irradiated as in (C), and the fraction of cells in G2 phase was determined by flow cytometry. The graph is a summary from two experiments. Error bars, SE.

DSBs (Figures 1B and S1E). The gene encoding RNF168 (RING finger protein 168) is located on chromosome 3 (3q29) and displays structural hallmarks of a RING finger ubiquitin ligase (Figure 1C). In addition to the RING domain, RNF168 possesses two motifs interacting with ubiquitin (MIU) known to bind polyubiquitin chains (Penengo et al., 2006).

Having identified RNF168 in a screen, we tested whether it regulates 53BP1 after the standard clastogen-induced DNA breakage. Indeed, the accumulation of 53BP1 in IR-induced foci was inhibited after knocking down RNF168 either by transient transfection of siRNA (Figures 1D, 1E, and S2A) or by inducing stably integrated shRNA (Figures 1D and S2B). This was achieved by several independent siRNAs targeting distinct regions of RNF168 mRNA (Figures 1E and S2A), and the 53BP1 accumulation at DSBs was rescued by the RNAi-resistant form of GFP-RNF168 (Figure 1F). Importantly, the latter experiments revealed that RNF168 itself accumulated at the DSB foci (Figure 1F, bottom panel). Together, these data identified RNF168 as a candidate regulator of the DSB-induced chromatin response, and we set out to investigate the underlying mechanisms.

RNF168 Regulates DSB-Associated Ubiquitylation and Accumulation of a Subset of Repair Proteins

We and others have recently described RNF8, a RING domain E3 ligase, which, by promoting local chromatin ubiquitylation, triggers the accumulation of several repair complexes, including 53BP1 (see Introduction). To test whether RNF168 is integrated in or operates in parallel to this pathway, we irradiated cells by a microlaser under conditions that generate limited amounts of DNA strand breaks in defined nuclear volumes (Bekker-Jensen et al., 2006; Lukas et al., 2003). Under these conditions, knockdown of RNF168 had no measurable effect on the extent of H2AX phosphorylation and accumulation of MDC1 and NBS1 (Figures 2A and S3), consistent with our previous findings that these initial steps of the DSB response do not require ubiquitylation (Mailand et al., 2007). Strikingly, however, although the recruitment of RNF8 was also normal in RNF168-depleted cells, the accumulation of conjugated ubiquitin at the DSB sites was severely

impaired (Figures 2A and S3). Thus, downregulation of RNF168 created a situation in which RNF8 accumulated at the sites of DNA damage, yet it was unable to sustain local chromatin ubiquitylation. Consequently, 53BP1 and BRCA1, two repair factors whose retention on damaged chromosomes requires ubiquitin (see Introduction), were unable to accumulate at the micro-laser-generated DSB tracks in the RNF168-deficient cells (Figures 2A and S3), consistent with the lack of 53BP1 retention at IR-induced nuclear foci observed earlier in RNF168-deficient cells (see Figures 1E, 1F, S2A, and S2B). Together, RNF168 emerged from these experiments as a novel factor, which operates downstream of RNF8 and is required for sustained ubiquitylation of the DSB sites and accumulation of a subset of genome caretakers on damaged chromosomes.

Knockdown of RNF168 Delays Recovery from Genotoxic Stress

To test the significance of the RNF168-controlled events for the DNA damage response, we silenced endogenous RNF168 in U-2-OS cells by RNAi, exposed these cells to a moderate dose of IR, and followed in time the MDC1-decorated DSB foci in individual nuclei. Because MDC1 operates upstream of the ubiquitin-dependent steps during the DSB-induced chromatin response (Figure 2A), it can serve as a sensitive indicator of the DSB dynamics even in the absence of the DNA damage-associated E3 ligases. The number of nuclei with MDC1 foci detected early (1 hr) after IR was very similar in control and RNF168-deficient cells (92% and 98%, respectively). However, while in control cells, MDC1 progressively dissociated from DSBs (consistent with the ongoing DNA repair), knockdown of RNF168 caused marked persistence of the MDC1 foci even at the time points when the control cells returned to the predamage values (Figures 2B and S4). This suggested delayed dynamics of the DSB repair in RNF168-deficient cells, a notion that was further supported by a prolonged phosphorylation of NBS1 and SMC1 (two genome caretakers targeted by ATM after DNA damage) (Figure 2C), and by an extended IR-induced G2 arrest (Figure 2D). Based on these results, we conclude that RNF168 facilitates restoration of genome integrity challenged by DSBs.

Assembly of RNF168 at DSBs Is Mediated by Its Ubiquitin-Binding Domains

To mechanistically elucidate RNF168 function, we turned to the earlier observation that RNF168, when ectopically expressed, concentrated in the IR-induced nuclear foci (see Figure 1F). We could extend this result by showing that also endogenous RNF168 accumulates at DSBs generated either by the laser microirradiation (Figures 3A, top panel, and 4A) or IR (Figures 4C and 4D). Of note, RNF168 localized to the broad, γ-H2AX-decorated chromosomal regions (see insets in Figures 4A and S5A) throughout the interphase (Figure S5B), consistent with the emerging evidence that the formation of the DSB-flanking chromatin compartment is cell-cycle independent (Bekker-Jensen et al., 2006; Mailand et al., 2007).

To understand the structural underpinnings of the RNF168-chromatin interaction, we silenced endogenous RNF168 by siRNA, reintroduced into these cells various forms of YFP-tagged (and siRNA-resistant) RNF168, and tested their ability to accumulate at the DSB sites. Both wild-type RNF168 and its variant bearing an inactivating mutation in the catalytic RING domain (*RING) avidly accumulated at DSBs (Figure 3B). In contrast, simultaneous mutations of both MIU domains (**MIU) attenuated retention of RNF168 at the DSB sites (Figure 3B), especially in cells with low levels of MIU-deficient RNF168 (Figure 3B, "Low"). High overexpression of this mutant was still compatible with some DSB retention, yet a substantial fraction of the protein always remained dispersed in the nucleoplasm, indicating a weakened affinity to damaged chromosomes (Figure 3B, "High"). Indeed, a rigorous measurement of protein mobility by fluorescence recovery after photobleacing (FRAP) revealed that the mean residence time, which wild-type RNF168 spent bound to DSB (11.13 $\pm$ 0.22 s), decreased nearly 5-fold (to 2.47 $\pm$ 0.07 s) in the double-MIU mutant (Figure 3C). These results suggested that the ubiquitin-binding domains contribute to the retention of RNF168 at DSBs, and this was further supported by the observation that a short inhibition of the 26S proteasome under conditions that disrupt chromatin-associated ubiquitin conjugates (Dantuma et al., 2006) prevented accumulation of RNF168 at DSBs (Figure 3A, bottom panel).

Maturation of the DSB-Flanking Chromatin Requires Catalytic and Ubiquitin-Binding Domains of RNF168

Because the above complementation assays were performed in cells with silenced endogenous RNF168, they allowed us to test the impact of RNF168 structural domains on ubiquitylation of the DSB-flanking chromatin and retention of repair proteins in this compartment (a process that we have recently dubbed as "maturation of the DSB-flanking chromatin") (Mailand et al., 2007). Strikingly, whereas cells complemented with wild-type RNF168 regained the ability to generate ubiquitin conjugates at the DSB sites (Figure 3B, top panel), both the *RING mutant (able to assemble at DSBs but impaired in its E3 ligase activity) (Figure 3B, middle panel) and the moderate levels of the **MIU mutant (active but deficient in DSB interaction) (Figure 3B, bottom panels, "Low") failed to rescue DSB ubiquitylation.

In the latter case, we noticed that massive overexpression of MIU-deficient RNF168 did induce some DSB-associated ubiquitylation (Figure 3B, bottom panels, "High"). Because such extreme levels appear to subvert natural requirements for RNF168 interaction with damaged chromatin, we wanted to quantify more exactly, and under more physiological conditions, the function of the MIU domains. We generated cell lines stably expressing moderately elevated wild-type or MIU-deficient versions of RNF168, both tagged with GFP and rendered RNAi insensitive (Figure S6A). After silencing the endogenous RNF168, the wild-type GFP-RNF168 avidly accumulated at the laser-generated DSB sites and induced massive ubiquitylation in this compartment (Figure 3D). In contrast, the MIU-deficient RNF168, expressed to a very similar level as the wild-type protein (Figure S6A), accumulated poorly and was significantly impaired in generating ubiquitin conjugates at the DSB-flanking chromatin (Figure 3D). These results were exactly mirrored in an assay in which we measured retention of 53BP1, a sensitive surrogate of DSB-associated ubiquitylation (see Introduction). Also here, the wild-type GFP-RNF168, but not the MIU-deficient

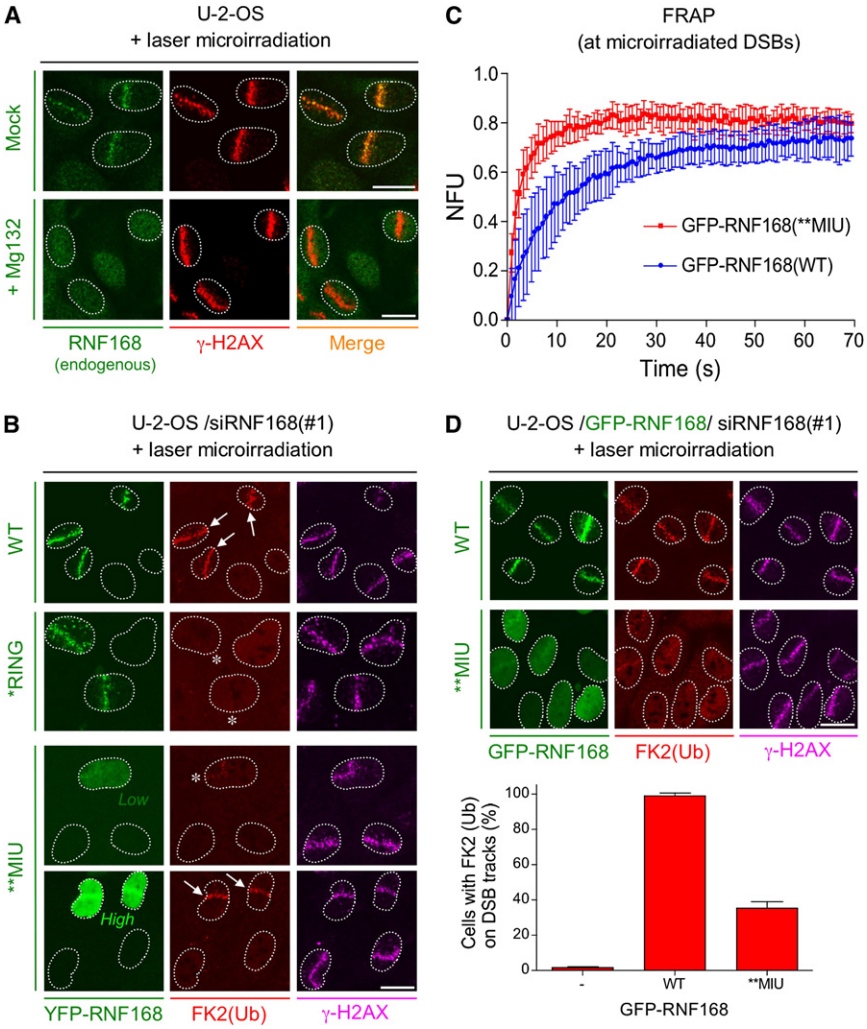

Figure 3. Assembly and Function of RNF168 at the DSB Sites Is Facilitated by Its Ubiquitin-Binding Domains

(A) U-2-OS cells were microirradiated, incubated for 1 hr, and immunostained with the indicated antibodies. Where indicated, the cells were incubated for 90 min with MG132 (5 μM) before microirradiation. The lack of RNF168 accumulation at DSBs in the Mg132-treated cells was observed in more than 100 microirradiated cells.

(B) U-2-OS cells were treated with the RNF168-targeting siRNA (#1) for 24 hr, transfected with the indicated RNAi-resistant RNF168 constructs, incubated for 24 hr, microirradiated, incubated for an additional 1 hr, and coimmunostained with antibodies to conjugated ubiquitin (FK2) and γ-H2AX. At least 50 cells in each condition showed consistent results. Arrows mark the cells in which the transgene expression restored DSB ubiquitylation; asterisks indicate cells with inefficient DSB ubiquitylation.

(C) U-2-OS cells were transfected with the indicated forms of GFP-RNF168, incubated for 24 hr, and microirradiated as in (B). At 1 hr later, the exchange rate of the GFP-tagged proteins at the DSB sites was determined by FRAP. The FRAP curves were derived from ten cells for each condition. NFU, normalized fluorescence units. Error bars, SE.

(D) U-2-OS cell lines stably expressing the indicated versions of RNAi-resistant GFP-RNF168 were microirradiated and immunostained as in (B). The microirradiated cells were scored for the presence of conjugated ubiquitin at the DSB tracks. The images (top) show representative fields; the graph (bottom) is a summary of two independent experiments in which at least 50 cells for each category were scored. Error bars, SE. Scale bars, 10 μm.

mutant, efficiently restored accumulation of 53BP1, both at the laser-generated DSB tracks (Figure S7A) and in the IR-induced nuclear foci (Figure S7B). Thus, we conclude that the maturation of the DSB-flanking chromatin is facilitated by the ubiquitin-dependent recruitment of RNF168 into this compartment.

Recruitment of RNF168 to DSBs Requires RNF8

One potential explanation for the MIU-mediated accumulation of RNF168 at DSBs would be if RNF168 could trigger its own recruitment by catalyzing local chromatin ubiquitylation. This, however, seemed unlikely because the RING-deficient form of RNF168 could still accumulate at the DSB sites (see Figure 3B). Therefore, we tested whether the recruitment of RNF168 to DSBs requires RNF8 or BRCA1, the other two E3 ligases known to associate with the DSB-flanking chromatin. Whereas knockdown of BRCA1 had no measurable effect, downregulation of RNF8 inhibited RNF168 accumulation at DSBs (Figure 4A). Consistently, knockdown of MDC1, the upstream regulator of RNF8, also prevented accumulation of RNF168 in this compartment (Figure 4A). Because the knockdown of MDC1 or RNF8 did not alter the total levels of endogenous RNF168 (Figure S6B), we conclude that the MDC1/RNF8 pathway regulates the RNF168 recruitment to the DSB compartment. Interestingly, knockdown of RNF8 did not alter the mobility of GFP-RNF168 in the undamaged nucleoplasm (Figure S8), indicating that the functional interplay between RNF8 and RNF168 is restricted to the sites of DNA damage.

To explore the hierarchy with which the distinct E3 ligases accumulate at DSBs in vivo, we subjected microirradiated cells stably expressing moderate levels of GFP-tagged RNF8, RNF168, or BRCA1 (Figures S6A and S9 and see Mailand et al., 2007) to a time-lapse microscopy and determined the time (t1/2) when a given protein reached half-maximum of its saturation in the DSB compartment (Lukas et al., 2004a and see Supplemental Experimental Procedures). These measurements revealed that each E3 ligase accumulated with distinct dynamics (Figures 4B and S9). Thus, the fastest protein to assemble at DSBs was RNF8 (t1/2 = 1.15 min), followed by RNF168 (t1/2 = 2.21 min), and only then by BRCA1 (t1/2 = 3.40 min). Collectively, these in vivo measurements supported the above genetic analysis and suggested that RNF168 operates downstream of RNF8 but upstream of BRCA1.

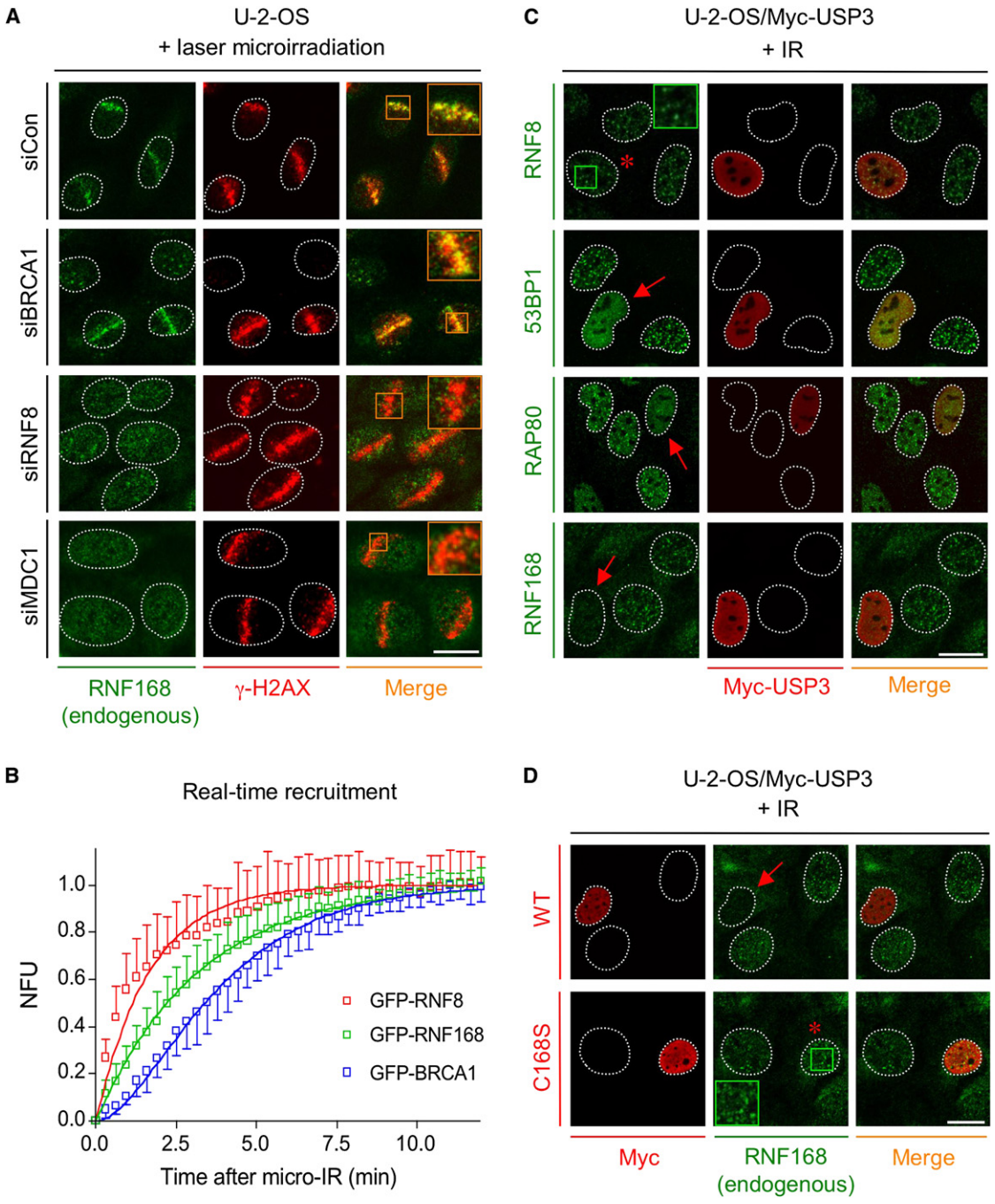

Figure 4. Requirements and Dynamics of RNF168 Accumulation at the DSB Sites

(A) U-2-OS cells were treated with the siRNAs indicated on the left for 3 days, microirradiated, and immunostained with the indicated antibodies. At least 100 microirradiated cells were scored for each siRNA treatment and showed consistent results.

(B) U-2-OS cells stably expressing the indicated GFP-tagged proteins were microirradiated, and the GFP-associated fluorescence intensities in the DSB tracks were recorded by real-time imaging until they stabilized. Kinetic curves were determined from ten cells for each protein. NFU, normalized fluorescence units. Error bars, SE.

(C) U-2-OS cells were transfected with the expression plasmid for Myc-USP3 for 24 hr, exposed to IR (4 Gy), and 1 hr later immunostained with the indicated antibodies. Arrows mark cells in which overexpression of Myc-USP3 prevented IR-induced focus formation of 53BP1, RAP80, and RNF168, respectively. Asterisk marks a cell in which Myc-USP3 did not impair RNF8 focus formation.

(D) U-2-OS cells were transfected with plasmids for wild-type (WT) or catalytically inactive (C168S) forms of Myc-USP3, irradiated, and immunostained as in (C). Arrow marks a cell in which WT Myc-USP3 prevented IR-induced focus formation of RNF168; asterisk marks a cell in which inactive USP3 failed to suppress RNF168 foci. Scale bars, 10 μm.

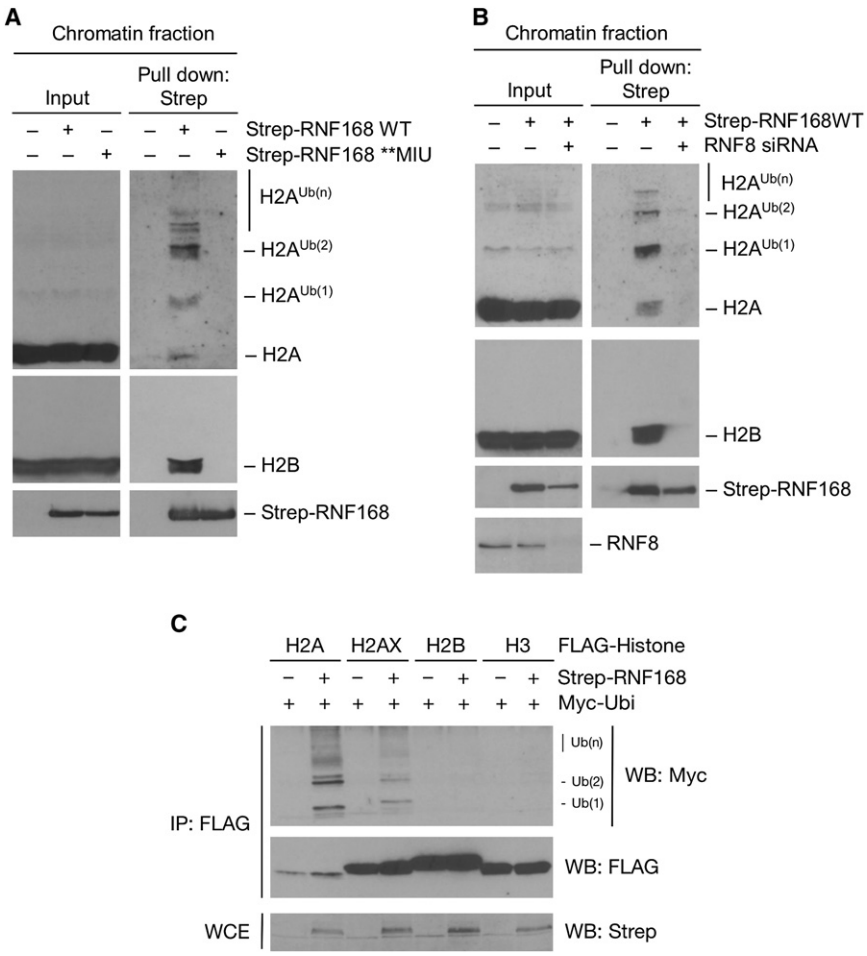

Figure 5. RNF168 Binds and Targets for Ubiquitylation a Subset of Histones

(A) 293T cells were transfected with the indicated versions of Strep-RNF168 and after 24 hr exposed to IR (10 Gy). At 1 hr later, the chromatin fractions were isolated, and the Strep-containing complexes were purified and analyzed by immunoblotting with the indicated antibodies.

(B) 293T cells were treated with RNF8 or control siRNAs for 48 hr, transfected with the Strep-RNF168 (WT) expression plasmid, incubated for 24 hr, irradiated (10 Gy), and 1 hr later analyzed as in (A).

(C) U-2-OS cells were cotransfected with the FLAG histones, Strep-RNF8, and Myc-Ubiquitin expression plasmids as indicated, incubated for 24 hr, lysed in denaturing buffer, and subjected to immunoprecipitation with anti-FLAG agarose beads under denaturing conditions. Bound complexes were analyzed by immunoblotting with the indicated antibodies.

Retention of RNF168 at DSBs Is Mediated by Ubiquitylated H2A

We next set out to elucidate how RNF8 promotes RNF168 chromatin retention. We have recently shown that H2A can be ubiquitylated by RNF8 in vitro and that both basal and DNA damage-induced H2A ubiquitylations are influenced by RNF8 in cells (Mailand et al., 2007). Another recent study identified USP3 as a deubiquitylating enzyme capable of reverting H2A ubiquitylation (Nicassio et al., 2007), suggesting that USP3 and RNF8 operate, at least in part, as opposing enzymatic activities. Indeed, we could support this concept by showing that, while overexpression of USP3 had no effect on the DSB retention of RNF8 itself, it abolished the IR-induced focus formation of 53BP1 and RAP80, two chromatin-binding factors whose retention at the DSB sites requires RNF8 (Figure 4C). But most significantly in this context, overexpression of wild-type USP3, but not its catalytically inactive mutant, prevented the IR-induced focus formation of RNF168 (Figures 4C and 4D), indicating that the assembly of RNF168 at DSBs requires H2A ubiquitylation.

The latter conclusion was further supported by a biochemical analysis of chromatin-enriched fractions from irradiated 293T cells expressing various forms of Strep-tagged RNF168. Whereas the wild-type RNF168 avidly bound to mono-, di-, and, to some extent, even polyubiquitylated H2A, the disruption of both MIU motifs abolished this interaction (Figure 5A). This was reflected by the ability of the wild-type, but not the MIU-deficient version of RNF168, to copurify with nucleosomes (exemplified by the core histone H2B in Figure 5A). Of note, the comparison of the abundance of H2A and H2B in these fractions revealed that RNF168 bound poorly to unmodified H2A (Figure 5A), indicating that the RNF168-containing complexes preferentially contained nucleosomes enriched in ubiquitylated H2A. Importantly, in a complementary experiment, knockdown of RNF8 markedly decreased the chromatin-bound fraction of wild-type RNF168 (Figure 5B). Together, these data suggested that RNF8-mediated ubiquitylation of H2A generates a docking signal for RNF168.

RNF168 Ubiquitylates H2A and H2AX and Triggers Generation of Lysine 63-Linked Ubiquitin Conjugates

Having established the hierarchy in the RNF8 and RNF168 assembly at the DSB sites, we set out to investigate how these two E3 ligases cooperate in increasing local chromatin ubiquitylation. To this end, we tested, by an in vivo ubiquitylation assay, whether RNF168 can target various histones (Mailand et al., 2007) and found that RNF168 efficiently ubiquitylated H2A and H2AX, but not H2B or H3 (Figure 5C). The striking ramification of this result was that the substrate specificity of RNF168 under these conditions was very similar to the one described earlier for RNF8 (Mailand et al., 2007), suggesting that RNF168 may stabilize and/or increase histone modifications initiated by RNF8.

It has been reported that RNF8 forms an active holoenzyme with UBC13, the only known E2 ubiquitin-conjugating enzyme capable of generating the lysine 63 (K63)-linked ubiquitin chains

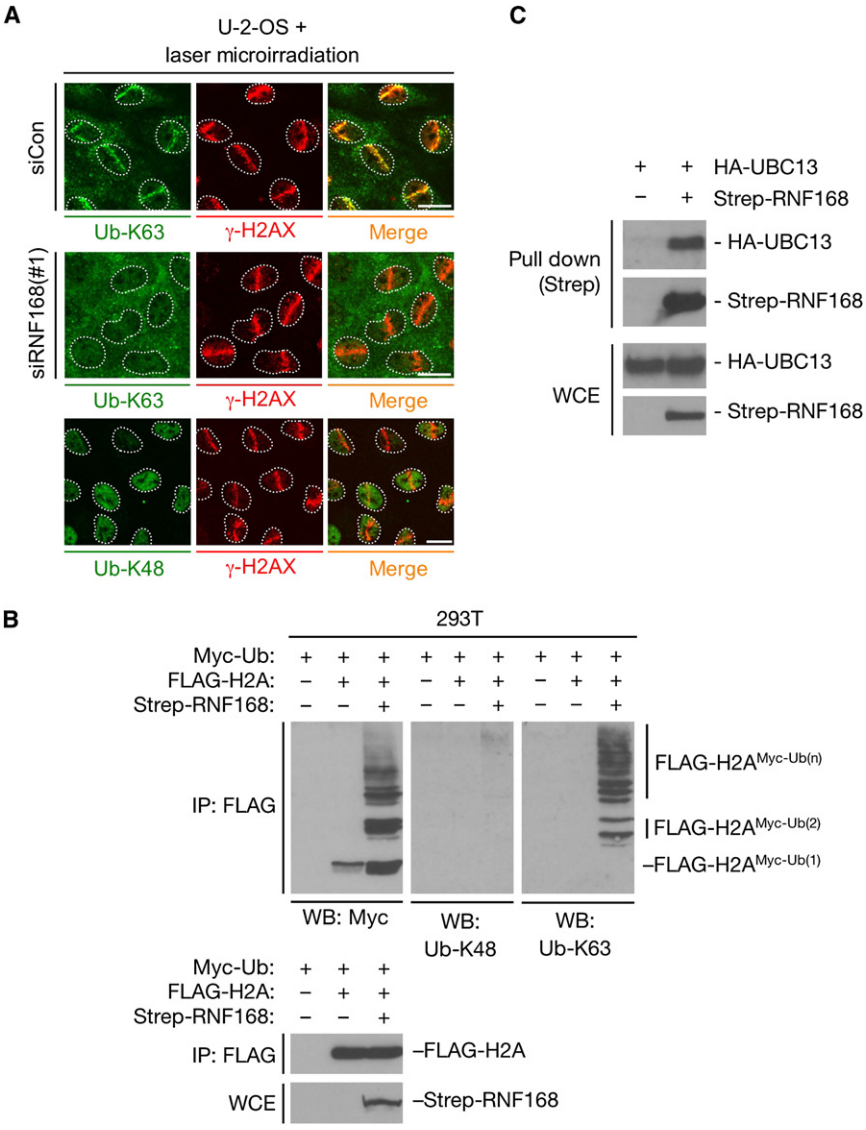

Figure 6. RNF168 Binds UBC13 and Catalyzes Formation of K63-Linked Ubiquitin Chains

(A) U-2-OS cells were microirradiated and 1 hr later immunostained with antibodies to K63- or K48-linked ubiquitin conjugates as indicated. All cells we coimmunostained with an antibody to γ-H2AX to detect the DSB tracks. Where indicated, cells were treated with control (siCon)- or RNF168 (#1)-targeting siRNAs for 2 days before microirradiation. At least 100 microirradiated cells were scored for each condition and showed consistent results. Scale bars, 10 μm.

(B) The 293 cells were cotransfected with the indicated constructs, subjected to anti-FLAG immunoprecipitation under denaturing conditions as in Figure 5C, and analyzed by immunoblotting with antibodies to the Myc-tag and the K63- or K48-linked ubiquitin conjugates. The immunoblotting in the bottom panel is a control for expression of FLAG-H2A and Strep-RNF168, respectively.

(C) U-2-OS cells were cotransfected with the HA-UBC13 and Strep-RNF168 constructs. After 24 hr, the Strep complexes were purified and analyzed by immunoblotting with the indicated antibodies. WCE, whole-cell extracts.

(Plans et al., 2006). Consistently, by means of overexpressing various lysine-deficient ubiquitin mutants, a recent study reported preferential accumulation of K63-linked ubiquitin polymers at the IR-induced nuclear foci (Sobhian et al., 2007). Stimulated by these findings, we reasoned that, if RNF168 propagated the RNF8 signaling, it should be able to generate K63-linked ubiquitin chains at the DSB-modified chromatin. To test this, we immunostained microirradiated cells with the linkage-specific antibodies that discriminate ubiquitin chains joined by K63 and K48, respectively (Newton et al., 2008). Indeed, whereas the anti-K63 linkage antibody robustly decorated the laser-generated DSB tracks (Figure 6A, top panel), no K48-linked ubiquitin chains were detected under these conditions (Figure 6A, bottom panel), and the accumulation of K63-linked ubiquitin was completely abrogated by knocking down endogenous RNF168 (Figure 6A, middle panel). Importantly, we were able to complement these results by an in vivo ubiquitylation assay, which revealed that the RNF168-induced ubiquitylation of H2A largely contained K63-linked, but not K48-linked, ubiquitin chains (Figure 6B). Although the latter results were obtained by overexpressed proteins, the fact that knocking down of endogenous RNF168 prevented accumulation of K63 ubiquitin linkages at DSBs in cells (see Figure 6A) strongly suggests that RNF168 catalyzes formation of this type of ubiquitin chains on damaged chromatin. Consistently, we could show that RNF168 and UBC13 physically interacted in cells (Figure 6C).

Interestingly, by a meticulous monitoring of the DSB-associated ubiquitylations during the first 10 min after DNA damage, we found that the temporal accumulation of conjugated ubiquitin at DSBs tightly correlated with the retention of RNF168 in this compartment (Figure S10A) and that no increase in local ubiquitin concentration was observed in cells with depleted RNF168, even in the earliest time points (Figure S10B). These data further supported the hypothesis that the ubiquitin conjugates generated by RNF8 are transient and/or unstable and require amplification and/or stabilization by RNF168 to achieve the threshold needed for the completion of the DSB-induced chromatin response.

RNF8 and RNF168 Constitute a Pathway Required for Efficient Cellular Responses to Genotoxic Stress

Finally, to address whether RNF8 and RNF168 operate along a common pathway, we combined treatment of cells by ionizing radiation with a protocol allowing us to genetically manipulate

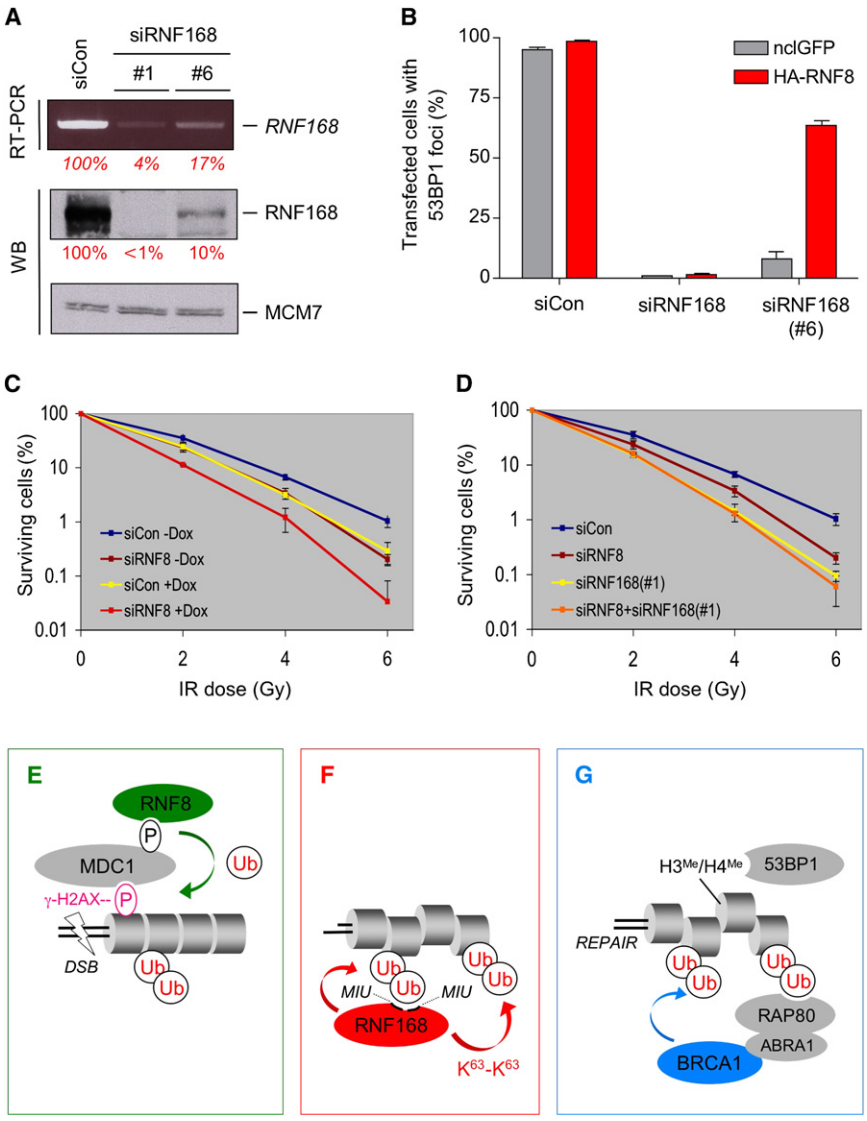

Figure 7. RNF168 and RNF8 Cooperate to Promote Chromatin Retention of 53BP1 and to Protect Cells against DSB-Generating Insults

(A) U-2-OS cells were treated with a control siRNA (siCon) or two distinct RNF168-targeting siRNAs (#1 and #6, respectively). After 2 days, RNA and proteins were extracted and subjected to RT-PCR (top) and western blot (WB) analysis (bottom). The relative abundance of RNF168 mRNA and protein for each treatment is indicated in red. MCM7 is a loading control.

(B) U-2-OS cells were treated by the indicated siRNAs as in (A) and after 24 hr transfected with a control (nuclear GFP; nclGFP) or HA-tagged RNF8 (HA-RNF8) expression plasmids. After 24 hr, the cells were exposed to IR (4 Gy), incubated for 1 hr, immunostained with the indicated antibodies, and scored for the IR-induced 53BP1 foci. The graph is a summary from two experiments in which at least 100 cells for each category were scored.

(C) The U-2-OS cell line conditionally expressing RNF168-targeting shRNA (U-2-OS/shRNA#1.2) was transfected with the indicated siRNAs and 1 day later induced or not by Doxycycline (Dox). After 2 days, the cells were split by the limiting dilution, incubated for an additional 1 day in the medium with or without Dox, and exposed to the indicated doses of IR. After 11 days, the dishes were stained with crystal violet, and the colonies with more than 50 cells were counted. Three independent experiments were performed, each with triplicate samples. The survival defects in RNF168-depleted cells were highly significant (see also Supplemental Experimental Procedures for the statistical analysis).

(D) U-2-OS cells (the same strain as in [C] but without induction) were transfected with the indicated siRNAs and subjected to the clonogenic survival assay as in (C). The efficiencies of si/shRNA downregulation for experiments in (B–D) are shown in Figures 1D and 7A (RNF168) and 5B (RNF8).

(B–D) Error bars, SE.

(E–G) A hypothetical model of ubiquitylation cascade within the DSB-modified chromatin compartment. See Discussion for details.

the "dosage" of RNF168. Specifically, we tested numerous RNF168-targetting siRNA oligonucleotides until we found a pair in which one siRNA (labeled as "#1") induced a robust downregulation of RNF168 at both mRNA and protein levels (Figure 7A, lane 2), whereas the other (labeled as "#6," targeting the 3′ untranslated region) reduced the RNF168 expression less efficiently (Figure 7A, lane 3). Importantly, the degree of RNF168 downregulation achieved by either of these siRNAs was sufficient to prevent any cytologically detectable retention of 53BP1 at the IR-induced nuclear foci (Figure 7B, gray bars; see also Figures 1E and S2A). We then overexpressed in these cells RNF8 and monitored the 53BP1 focus formation. Strikingly, whereas the elevated RNF8 was unable to support 53BP focus formation in cells with strongly depleted RNF168, it effectively induced 53BP1 foci in cells with a higher residual amount of RNF168 (Figures 7B and S11). These results suggested that, although RNF8 cannot "rescue" the near-to-complete absence of RNF168, the increased level of the former is able to cooperate with the residual amount of the latter to execute the DSB-induced chromatin response and promote retention of repair proteins in this compartment.

To independently test the emerging epistatic relationship between RNF8 and RNF168, we exploited an earlier observation that the cell line conditionally expressing the RNF168-targeting shRNA (shRNA#1.2) also contained more residual amount of RNF168 when compared to the strong siRNA oligonucleotide (siRNA#1) (see Figure 1D). Indeed, the clonogenic survival of irradiated cells after induction of the "milder" shRNA was better than after exposing the cells to the "stronger" siRNA (compare yellow lines in Figures 7C and 7D). But most importantly, while

the concomitant knockdown of RNF8 had no additive effect on IR sensitivity of cells with strongly depleted RNF168 (Figure 7D, yellow and orange lines), it significantly reduced survival in cells with less effective (''hypomorphic'') downregulation of RNF168 (Figure 7C, yellow and red lines). Thus, these data are consistent with a model in which RNF8 and RNF168 operate on a shared pathway that facilitates survival after genotoxic stress.

DISCUSSION

Our study reveals an unexpected complexity of how regulatory ubiquitylation orchestrates the chromatin response to DNA breakage (Figures 7E–7G). Although RNF8 is the first E3 ligase to assemble at the DSB-modified chromatin (Figure 7E), it is not sufficient to support sustained ubiquitylation. Instead, RNF8 appears to prime the DSB-modified chromatin for recruitment of RNF168, another E3 ligase (Figure 7F), whose activity is essential to amplify the initial DSB-associated ubiquitylations to a threshold required for the physiological function of this compartment (Figure 7G).

We can envisage two scenarios in which RNF168 increases local ubiquitylation at damaged chromosomes. First, it is possible that some targets of RNF168 overlap with those of RNF8. In such a scenario, RNF168 may not only amplify its own retention at the DSB-flanking chromatin, but also propagate the initial chromatin ubiquitylations (initiated by RNF8) to the neighboring nucleosomes. Indeed, our results provide several lines of evidence in support of such a model. Thus, we were able to show that both RNF8 and RNF168 target for ubiquitylation the same spectrum of histones (H2A and H2AX) (see Figure 5). In addition, we found that, like RNF8, RNF168 interacts with UBC13 and generates K63-linked ubiquitin chains (Figure 6). Furthermore, we provide evidence that, while neither of the two E3 ligases can execute the full DSB-induced chromatin response alone, the elevated levels of one (RNF8) cooperated with reduced levels of the other (RNF168) to trigger ubiquitin-dependent chromatin retention of 53BP1 (Figures 7A and 7B). Finally, by a reverse approach, we show that the moderate clonogenic survival defect in cells with incompletely silenced RNF168 can be augmented by codepletion of RNF8 (Figure 7C). Collectively, these results are consistent with an ''epistatic'' model in which the initial ubiquitin polymers generated by RNF8 are recognized by the ubiquitin-binding domain of RNF168 and then stabilized and/or amplified to generate an ''interaction trap'' for additional factors required for restoration of genome integrity (Figure 7E–7G).

There is also a second possibility, namely that RNF168 may extend the spectrum of the DSB-associated ubiquitylations by targeting unique substrate(s). Although we do not have direct evidence in support of this hypothesis, we by no means want to exclude it. Clearly, the key challenge for the future is to identify the spectrum of unique versus overlapping substrates of RNF8 and RNF168 E3 ligases, a task that, in order to solve this issue in full, would have to include systems biology approaches such as differential analysis of ubiquitylated proteomes in cells with genetically disrupted RNF8 and RNF168, respectively. Importantly, the above scenarios are not mutually exclusive, and both are compatible with our main conclusion, namely that the key function of RNF168 in genome surveillance is to increase chromatin ubiquitylation to the threshold required for retention of important repair factors such as 53BP1 or BRCA1. Interestingly, BRCA1 is also a RING domain E3 ligase, and there is evidence that cells with dysfunctional BRCA1 accumulate less-conjugated ubiquitin at the DSB sites (Polanowska et al., 2006). Thus, the maturation of the DSB-flanking chromatin can be viewed as a pathway initiated by RNF8, amplified by RNF168, and maintained by BRCA1 (Figures 7E–7G).

Such a concept has important ramifications. The sequential involvement of three ubiquitin ligases and, indeed, the massive accumulation of conjugated ubiquitin at the DSB-modified chromatin suggest that regulatory ubiquitylation represents a crucial posttranslational modification generated in the vicinity of these highly cytotoxic chromosomal lesions. Furthermore, the RNF8-RNF168-BRCA1 pathway can be viewed as an unprecedented type of functional interplay among the RING domain E3 ligases. Although the mutual crosstalk within the RING family of enzymes is well established, the known examples are almost exclusively based on the assembly of distinct RING domain proteins into larger supramolecular complexes required to generate fully functional holoenzymes (Buchwald et al., 2006). In contrast, we could not detect direct binding between RNF8 and RNF168, and BRCA1 did not seem to interact with either of the former proteins (our unpublished data). Instead, it seems that a ubiquitylation event catalyzed by the more upstream E3 ligase in this pathway triggers the recruitment of the downstream component, which can then amplify and/or maintain a high concentration of conjugated ubiquitin near the DSB lesions as long as it is needed for efficient repair (Figures 7E–7G).

Finally, whereas the sequential involvement of three E3 ligases provides an opportunity for a more subtle regulation of the DSB-induced chromatin response, it also broadens the target for potential mutations and subversion of this pathway in disease. Most notably in this regard, BRCA1 is an established tumor suppressor, whose mutations predispose to familial breast and ovarian cancer (Boulton, 2006). Furthermore, other studies underscored the importance of the ubiquitin-driven pathways for genomic stability by showing that inhibition of the proteasome (which, among other effects, impairs regulatory ubiquitylation in the nucleus) suppresses DNA repair by homologous recombination (Murakawa et al., 2007). Strikingly, the locus encoding RNF168, the upstream component of the BRCA1 ''assembly line,'' has been found mutated in the RIDDLE (radiosensitivity, immune deficiency, dysmorphic features, and learning difficulties) syndrome (Stewart et al., 2009 [this issue of *Cell*]). Thus, the RNF8-RNF168-BRCA1 cascade emerges as a target for mutations in genome instability disorders, and it would be important to test whether its alterations can explain the defects in hitherto elusive clinical cases with hallmarks of radiation sensitivity and/or increased incidence of genome instability.

EXPERIMENTAL PROCEDURES

Screen for 53BP1 Regulators

The screening procedure using the siRNA arrays was carried out as described (Erfle et al., 2007) with modifications specified in Figures S1A–S1G. Briefly, U-2-OS cells were seeded on the siRNA arrays, incubated for 3 days,

immunostained with antibodies to 53BP1, and analyzed by high-content microscopy for the retention of 53BP1 in the intranuclear foci. The complete screening procedure is described in the Supplemental Experimental Procedures.

Plasmids, PCR, and RNA Interference

The cDNA for human RNF168, tagged on the N terminus by YFP, was obtained from Imagenes (http://www.imagenes-bio.de/). The RNF168 ORF was rendered si/shRNA resistant by introducing silent mutations specified in the Supplemental Experimental Procedures. The point mutations in the RING domain (*RING; C16S) and the MIU domains (**MIU; A179G-A450G) (Penengo et al., 2006) were generated using the QuickChange Site-Directed Mutagenesis Kit (Stratagene). The GFP-, GST-, and Strep-tagged versions of RNF168 were generated by subcloning the respective cDNAs into the pAcGFP-C1 (Clontech), pGEX-6P (Amersham Biosciences), and pEXPR-103 (IBA BioTAGnology), respectively. The cDNA for USP3 was obtained from Imagenes; the mutation in its catalytic site (C168S) was generated by site-directed mutagenesis and subcloned into pcDNA3-Myc (Invitrogen). The expression plasmid for HA-RNF8 was described (Mailand et al., 2007). The plasmid for HA-Ubc13 (pEF-HA-Ubc13) was a gift from Dr. Ze'ev Ronai. For RT-PCR, RNA was extracted by the RNeasy Mini Kit (Invitrogen), and the PCR reaction was performed by One Step RT PCR Kit (QIAGEN) with primers specified in the Supplemental Experimental Procedures. Plasmid transfections were performed using FuGene 6 (Roche Molecular Biochemicals). All siRNA transfections were performed with 100 nM siRNA duplexes using Lipofectamine RNAiMAX (Invitrogen) and with oligonucleotide sequences specified in the Supplemental Experimental Procedures.

Cell Culture and Generation of DSBs

Human U-2-OS osteosarcoma cells and 293T human embryonic kidney cells were grown in DMEM containing 10% fetal bovine serum (GIBCO). U-2-OS cell lines expressing GFP-RNF8 and GFP-BRCA1 were described (Mailand et al., 2007). U-2-OS cell lines expressing various forms of GFP-RNF168 are characterized in Figure S6A. U-2-OS cell lines expressing the RNF168-targeting shRNA in a Doxycycline-inducible manner were generated with oligonucleotides specified in the Supplemental Experimental Procedures and induced as in Mailand et al. (2006). Flow cytometry was performed as in Sorensen et al. (2000). Survival curves in clonogenic assays were analyzed using the linear quadratic model for the relationship between cell survival and radiation dosage: $Ln(SF) = \alpha D + \beta D^2$, in which SF is the survival fraction, and D is the radiation dose. Comparison of the survival curves for different treatments was performed as described (Franken et al., 2006). IR was delivered by the X-ray generator (Pantak HF160, 150 kV, 15 mA, dose rate 2.18 Gy/min). Laser microirradiation and conditions for time-lapse microscopy were described (Bekker-Jensen et al., 2006; Lukas et al., 2003, 2004a).

Immunochemical and Biochemical Methods

Rabbit antibody to RNF168 is characterized in the accompanying paper by Stewart et al. (2009). The linkage-specific antibodies to K63 (Apu3.A8) or K48 (Apu2.07) ubiquitin conjugates were provided by Kim Newton and Vishva M. Dixit (Genentech) (Newton et al., 2008). Antibodies to MDC1, RNF8, and 53BP1 were gifts from Drs. Stephen Jackson, Junjie Chen, and Thanos Halazonetis, respectively. Commercially available antibodies are specified in the Supplemental Experimental Procedures. Conditions for immunoprecipitation, immunoblotting, and immunofluorescence were described (Bekker-Jensen et al., 2006; Mailand et al., 2006). Preparation of chromatin-enriched fractions and conditions for in vivo ubiquitylation were described (Mailand et al., 2007). Strep-tagged RNF168 protein complexes were purified on Strep-Taction Sepharose (IBA BioTAGnology) according to the manufacturer's instructions.

Microscopy

Confocal images were acquired on LSM-510 (Carl Zeiss Microimaging Inc.) mounted on an upright Zeiss-Axioimager, equipped with an oil-immersion objective (Plan-Apochromat 40×/1.3). Image analysis procedures, real-time recruitment assays, and quantitative photobleaching techniques (covering both screening and experimental parts of this study) are described in detail in the Supplemental Experimental Procedures.

ACCESSION NUMBERS

The Ensembl accession number for the RNF168 sequence reported in this paper is ENSG00000163961.

SUPPLEMENTAL DATA

The Supplemental Data include Supplemental Experimental Procedures and 11 figures and can be found with this article online at http://www.cell.com/supplemental/S0092-8674(09)00004-X.

ACKNOWLEDGMENTS

We thank Junjie Chen, Stephen Jackson, Thanos Halazonetis, Ze'ev Ronai, Kim Newton, and Vishva M. Dixit for reagents; Mark R. Payne for help with statistical analysis; and Holger Erfle and Beate Neumann for assistance with the siRNA screen. This work was supported by the Danish Cancer Society, Danish National Research Foundation, European Commission Integrated Projects "DNA Repair" and "GENICA," Lundbeck Foundation (R13-A1287), Danish Research Council, and the John and Birthe Meyer Foundation. J.E. and R.P. acknowledge support from the German Federal Ministry of Education and Research (BMBF) grant within the National Genome Research Network (NGFN-1, SMP-RNAi, 01GR0403) and the European Commission Integrated Project Mitocheck (FP6-503464).

Received: July 3, 2008
Revised: October 17, 2008
Accepted: December 17, 2008
Published: February 5, 2009

REFERENCES

Bekker-Jensen, S., Lukas, C., Kitagawa, R., Melander, F., Kastan, M.B., Bartek, J., and Lukas, J. (2006). Spatial organization of the Mamm. Genome surveillance machinery in response to DNA strand breaks. J. Cell Biol. *173*, 195–206.

Bonilla, C.Y., Melo, J.A., and Toczyski, D.P. (2008). Colocalization of sensors is sufficient to activate the DNA damage checkpoint in the absence of damage. Mol. Cell *30*, 267–276.

Botuyan, M.V., Lee, J., Ward, I.M., Kim, J.E., Thompson, J.R., Chen, J., and Mer, G. (2006). Structural basis for the methylation state-specific recognition of histone H4-K20 by 53BP1 and Crb2 in DNA repair. Cell *127*, 1361–1373.

Boulton, S.J. (2006). Cellular functions of the BRCA tumour-suppressor proteins. Biochem. Soc. Trans. *34*, 633–645.

Buchwald, G., van der Stoop, P., Weichenrieder, O., Perrakis, A., van Lohuizen, M., and Sixma, T.K. (2006). Structure and E3-ligase activity of the Ring-Ring complex of polycomb proteins Bmi1 and Ring1b. EMBO J. *25*, 2465–2474.

Celeste, A., Difilippantonio, S., Difilippantonio, M.J., Fernandez-Capetillo, O., Pilch, D.R., Sedelnikova, O.A., Eckhaus, M., Ried, T., Bonner, W.M., and Nussenzweig, A. (2003). H2AX haploinsufficiency modifies genomic stability and tumor susceptibility. Cell *114*, 371–383.

Dantuma, N.P., Groothuis, T.A., Salomons, F.A., and Neefjes, J. (2006). A dynamic ubiquitin equilibrium couples proteasomal activity to chromatin remodeling. J. Cell Biol. *173*, 19–26.

Erfle, H., Neumann, B., Liebel, U., Rogers, P., Held, M., Walter, T., Ellenberg, J., and Pepperkok, R. (2007). Reverse transfection on cell arrays for high content screening microscopy. Nat. Protoc. *2*, 392–399.

Fernandez-Capetillo, O., Lee, A., Nussenzweig, M., and Nussenzweig, A. (2004). H2AX: The histone guardian of the genome. DNA Repair (Amst.) *3*, 959–967.

Franken, N.A., Rodermond, H.M., Stap, J., Haveman, J., and van Bree, C. (2006). Clonogenic assay of cells in vitro. Nat. Protoc. *1*, 2315–2319.

Huen, M.S., Grant, R., Manke, I., Minn, K., Yu, X., Yaffe, M.B., and Chen, J. (2007). RNF8 transduces the DNA-damage signal via histone ubiquitylation and checkpoint protein assembly. Cell *131*, 901–914.

Huyen, Y., Zgheib, O., Ditullio, R.A., Jr., Gorgoulis, V.G., Zacharatos, P., Petty, T.J., Sheston, E.A., Mellert, H.S., Stavridi, E.S., and Halazonetis, T.D. (2004). Methylated lysine 79 of histone H3 targets 53BP1 to DNA double-strand breaks. Nature *432*, 406–411.

Ikura, T., Tashiro, S., Kakino, A., Shima, H., Jacob, N., Amunugama, R., Yoder, K., Izumi, S., Kuraoka, I., Tanaka, K., et al. (2007). DNA damage-dependent acetylation and ubiquitination of H2AX enhances chromatin dynamics. Mol. Cell. Biol. *27*, 7028–7040.

Kolas, N.K., Chapman, J.R., Nakada, S., Ylanko, J., Chahwan, R., Sweeney, F.D., Panier, S., Mendez, M., Wildenhain, J., Thomson, T.M., et al. (2007). Orchestration of the DNA-damage response by the RNF8 ubiquitin ligase. Science *318*, 1637–1640.

Lukas, C., Falck, J., Bartkova, J., Bartek, J., and Lukas, J. (2003). Distinct spatiotemporal dynamics of mammalian checkpoint regulators induced by DNA damage. Nat. Cell Biol. *5*, 255–260.

Lukas, C., Melander, F., Stucki, M., Falck, J., Bekker-Jensen, S., Goldberg, M., Lerenthal, Y., Jackson, S.P., Bartek, J., and Lukas, J. (2004a). Mdc1 couples DNA double-strand break recognition by Nbs1 with its H2AX-dependent chromatin retention. EMBO J. *23*, 2674–2683.

Lukas, J., Lukas, C., and Bartek, J. (2004b). Mammalian cell cycle checkpoints: Signalling pathways and their organization in space and time. DNA Repair (Amst.) *3*, 997–1007.

Mailand, N., Bekker-Jensen, S., Bartek, J., and Lukas, J. (2006). Destruction of Claspin by SCFbetaTrCP restrains Chk1 activation and facilitates recovery from genotoxic stress. Mol. Cell *23*, 307–318.

Mailand, N., Bekker-Jensen, S., Faustrup, H., Melander, F., Bartek, J., Lukas, C., and Lukas, J. (2007). RNF8 ubiquitylates histones at DNA double-strand breaks and promotes assembly of repair proteins. Cell *131*, 887–900.

Melander, F., Bekker-Jensen, S., Falck, J., Bartek, J., Mailand, N., and Lukas, J. (2008). Phosphorylation of SDT repeats in the MDC1 N terminus triggers retention of NBS1 at the DNA damage-modified chromatin. J. Cell Biol. *181*, 213–226.

Murakawa, Y., Sonoda, E., Barber, L.J., Zeng, W., Yokomori, K., Kimura, H., Niimi, A., Lehmann, A., Zhao, G.Y., Hochegger, H., et al. (2007). Inhibitors of the proteasome suppress homologous DNA recombination in mammalian cells. Cancer Res. *67*, 8536–8543.

Murr, R., Loizou, J.I., Yang, Y.G., Cuenin, C., Li, H., Wang, Z.Q., and Herceg, Z. (2006). Histone acetylation by Trrap-Tip60 modulates loading of repair proteins and repair of DNA double-strand breaks. Nat. Cell Biol. *8*, 91–99.

Newton, K., Matsumoto, M.L., Wertz, I.E., Kirkpatrick, D.S., Lill, J.R., Tan, J., Dugger, D., Gordon, N., Sidhu, S.S., Fellouse, F.A., et al. (2008). Ubiquitin chain editing revealed by polyubiquitin linkage-specific antibodies. Cell *134*, 668–678.

Nicassio, F., Corrado, N., Vissers, J.H., Areces, L.B., Bergink, S., Marteijn, J.A., Geverts, B., Houtsmuller, A.B., Vermeulen, W., Di Fiore, P.P., et al. (2007). Human USP3 is a chromatin modifier required for S phase progression and genome stability. Curr. Biol. *17*, 1972–1977.

Penengo, L., Mapelli, M., Murachelli, A.G., Confalonieri, S., Magri, L., Musacchio, A., Di Fiore, P.P., Polo, S., and Schneider, T.R. (2006). Crystal structure of the ubiquitin binding domains of rabex-5 reveals two modes of interaction with ubiquitin. Cell *124*, 1183–1195.

Plans, V., Scheper, J., Soler, M., Loukili, N., Okano, Y., and Thomson, T.M. (2006). The RING finger protein RNF8 recruits UBC13 for lysine 63-based self polyubiquitylation. J. Cell. Biochem. *97*, 572–582.

Polanowska, J., Martin, J.S., Garcia-Muse, T., Petalcorin, M.I., and Boulton, S.J. (2006). A conserved pathway to activate BRCA1-dependent ubiquitylation at DNA damage sites. EMBO J. *25*, 2178–2188.

Sobhian, B., Shao, G., Lilli, D.R., Culhane, A.C., Moreau, L.A., Xia, B., Livingston, D.M., and Greenberg, R.A. (2007). RAP80 targets BRCA1 to specific ubiquitin structures at DNA damage sites. Science *316*, 1198–1202.

Sorensen, C.S., Lukas, C., Kramer, E.R., Peters, J.M., Bartek, J., and Lukas, J. (2000). Nonperiodic activity of the human anaphase-promoting complex-Cdh1 ubiquitin ligase results in continuous DNA synthesis uncoupled from mitosis. Mol. Cell. Biol. *20*, 7613–7623.

Soutoglou, E., and Misteli, T. (2008). Activation of the cellular DNA damage response in the absence of DNA lesions. Science *320*, 1507–1510.

Spycher, C., Miller, E.S., Townsend, K., Pavic, L., Morrice, N.A., Janscak, P., Stewart, G.S., and Stucki, M. (2008). Constitutive phosphorylation of MDC1 physically links the MRE11-RAD50-NBS1 complex to damaged chromatin. J. Cell Biol. *181*, 227–240.

Stewart, G.S., Panier, S., Townsend, K., Al-Hakim, A.K., Kolas, N.K., Miller, E.S., Nakada, S., Ylanko, J., Olivarius, S., Mendez, M., et al. (2009). The RIDDLE syndrome protein mediates a ubiquitin-dependent signaling cascade at sites of DNA damage. Cell *136*, this issue, 420–434.

Stucki, M., Clapperton, J.A., Mohammad, D., Yaffe, M.B., Smerdon, S.J., and Jackson, S.P. (2005). MDC1 directly binds phosphorylated histone H2AX to regulate cellular responses to DNA double-strand breaks. Cell *123*, 1213–1226.

Wang, B., and Elledge, S.J. (2007). Ubc13/Rnf8 ubiquitin ligases control foci formation of the Rap80/Abraxas/Brca1/Brcc36 complex in response to DNA damage. Proc. Natl. Acad. Sci. USA *104*, 20759–20763.

Wang, B., Matsuoka, S., Ballif, B.A., Zhang, D., Smogorzewska, A., Gygi, S.P., and Elledge, S.J. (2007). Abraxas and RAP80 form a BRCA1 protein complex required for the DNA damage response. Science *316*, 1194–1198.

Yan, J., Kim, Y.S., Yang, X.P., Li, L.P., Liao, G., Xia, F., and Jetten, A.M. (2007). The ubiquitin-interacting motif containing protein RAP80 interacts with BRCA1 and functions in DNA damage repair response. Cancer Res. *67*, 6647–6656.